4SM Observations: Cryosphere Supplementary Material

Coordinating Lead Authors:
David G. Vaughan (UK), Josefino C. Comiso (USA)

Lead Authors:
Ian Allison (Australia), Jorge Carrasco (Chile), Georg Kaser (Austria/Italy), Ronald Kwok (USA), Philip Mote (USA), Tavi Murray (UK), Frank Paul (Switzerland/Germany), Jiawen Ren (China), Eric Rignot (USA), Olga Solomina (Russian Federation), Konrad Steffen (USA/Switzerland), Tingjun Zhang (USA/China)

Contributing Authors:
Anthony A. Arendt (USA), David B. Bahr (USA), Michiel van den Broeke (Netherlands), Ross Brown (Canada), J. Graham Cogley (Canada), Alex S. Gardner (USA), Sebastian Gerland (Norway), Stephan Gruber (Switzerland), Christian Haas (Canada), Jon Ove Hagen (Norway), Regine Hock (USA), David Holland (USA), Matthias Huss (Switzerland), Thorsten Markus (USA), Ben Marzeion (Austria), Rob Massom (Australia), Geir Moholdt (USA), Pier Paul Overduin (Germany), Antony Payne (UK), W. Tad Pfeffer (USA), Terry Prowse (Canada), Valentina Radić (Canada), David Robinson (USA), Martin Sharp (Canada), Nikolay Shiklomanov (USA), Sharon Smith (Canada), Sharon Stammerjohn (USA), Isabella Velicogna (USA), Peter Wadhams (UK), Anthony Worby (Australia), Lin Zhao (China)

Review Editors:
Jonathan Bamber (UK), Philippe Huybrechts (Belgium), Peter Lemke (Germany)

This chapter supplementary material should be cited as:
Vaughan, D.G., J.C. Comiso, I. Allison, J. Carrasco, G. Kaser, R. Kwok, P. Mote, T. Murray, F. Paul, J. Ren, E. Rignot, O. Solomina, K. Steffen and T. Zhang, 2013: Observations: Cryosphere Supplementary Material. In: *Climate Change 2013: The Physical Science Basis. Contribution of Working Group I to the Fifth Assessment Report of the Intergovernmental Panel on Climate Change* [Stocker, T.F., D. Qin, G.-K. Plattner, M. Tignor, S.K. Allen, J. Boschung, A. Nauels, Y. Xia, V. Bex and P.M. Midgley (eds.)]. Available from www.climatechange2013.org and www.ipcc.ch.

Table of Contents

4SM

4.SM.1 Supplementary Material for the Sea Ice Section

Most of the published studies on the large-scale variability and trends of the global sea ice cover that have been published in recent years were based primarily on results from analysis of passive microwave satellite data (Parkinson et al., 1999; e.g., Zwally et al., 2002; Stroeve et al., 2007; Comiso and Nishio, 2008; Stammerjohn et al., 2008; Cavalieri and Parkinson, 2012; Parkinson and Cavalieri, 2012)

The first satellite-borne imaging passive microwave sensor was the Nimbus-5/Electrically Scanning Microwave Radiometer (ESMR), which provided quantitative measurements of the extent and variability of the sea ice cover in both hemispheres from 1973 to 1976 (Zwally et al., 1983; Parkinson et al., 1987). However, with only one channel and a system that scanned a wide field of view (between –50 and +50 degrees off-nadir, causing changes in incidence angle and footprint size), gaps in the record from a few days to a few months and an unknown bias, these data have not been included in time series variability and trend analysis in Chapter 4.

The data that are most frequently used are those from the multichannel, conically scanning (i.e., constant incident angle) and dual polarized microwave radiometers that provide more accurate and more consistent ice concentration and hence ice extent and ice area (see Glossary for definitions) products. This series started with the Nimbus-7 Scanning Multichannel Microwave Radiometer (SMMR) which was launched in October 1978 and provided, for the first time, measurements that allowed unambiguous determination of sea ice concentration (Gloersen et al., 1993).

Several algorithms for deriving sea ice concentration using different techniques and utilizing different sets of channels have been developed (Svendsen et al., 1983; Cavalieri et al., 1984; Swift et al., 1985; Comiso, 1986; Steffen et al., 1992). The most commonly used techniques for sea ice studies are the Nimbus-7 National Aeronautics and Space Administration (NASA) Team algorithm (NT1, Cavalieri et al., 1984) and the Bootstrap algorithm (Comiso, 1986). SMMR was eventually succeeded by a series of Special Sensor Microwave/Imager (SSM/I) sensors and the two systems now provide a continuous set of data from November 1978 to the present. Subsequently, a more capable and improved sensor, Advanced Microwave Scanning Radiometer - Earth Observing System (AMSR-E), was launched on board the NASA/Aqua satellite and this has provided higher resolution and improved sea ice data from May 2002 to October 2011. The algorithms currently used for this sensor are the AMSR-E Bootstrap Algorithm (ABA) and the NASA Team Algorithm, Version 2 (NT2) as discussed in Markus and Cavalieri (2000). With some enhancements ABA was also adapted and used to reprocess SMMR and SSM/I data, and called SSM/I (or SMMR) Bootstrap Algorithm (SBA) as discussed in Comiso and Nishio (2008).

Using the SBA, AMSR-E data were used as the baseline and basis for improving the SMMR and SSM/I ice data sets used in Chapter 4. NT2 addressed some of the problems associated with NT1, such as erroneously low ice concentrations within the pack caused by unpredictable polarization ratios. Comparisons of NT2 and Bootstrap data have shown good agreement (Comiso and Parkinson, 2008; Parkinson and Comiso, 2008) in analyzed trends and variability. NT2 data, however, could not be used for the entire historical data because it requires the use of 89 GHz data, which is not available in SMMR and in the early part of the SSM/I time series. The time series that has been used as an alternative to the NT2 time series has thus been the NT1 time series which provides values different from NT2. In the meantime, the Hadley Centre, in collaboration with National Oceanic and Atmospheric Administration (NOAA), constructed another sea ice record referred to as HadISST_Ice. The data set has been assembled together with sea surface temperature (SST) at a relatively coarser resolution (1° latitude by 1° longitude) and for a longer time series. The data set as described in Rayner et al., (2003) made use of atlases, *in situ* data and ice centre data (as in, Walsh and Chapman, 2001) for the pre-satellite era. Starting in 1979, satellite data including those from NT1 have been used. The use of satellite data in the Hadley data set, however, apparently has had some problems of consistency because, apparently spurious, sudden increases in ice concentration from one year to another have been identified (e.g., Screen, 2011), making the data set difficult to use for variability and trend analysis. Also, as Screen (2011) pointed out, there are large differences in ice extent and ice area distributions derived from NT1 data compared with those derived from NT2 data.

The results presented in Section 4.2 make use of mainly SBA data for consistency with those presented in AR4. To assess the robustness of the conclusions of Section 4.2 to changes in the data sets used, a comparative analysis of results from SBA, NT1 and Hadley (i.e., HadISST1_Ice) data is presented.

Time series plots of monthly anomalies in ice extent as derived from SBA, NT1 and Hadley for the period November 1978 to December 2011 are presented in Figure 4.SM.1. Although data up to December 2012 are presented in Chapter 4, data available for HadISST1_Ice and NT1 for this comparison goes up to December 2011 only. The NT1 data set used is an update version of that presented in Cavalieri and Parkinson (2012) and Parkinson and Cavalieri (2012). The plots in Figure 4.SM.1a and 4.SM.1b for SBA and NT1, respectively show very similar patterns, but the Hadley plot (Figure 4.SM.1c) shows deviations from the other two, especially from 1984 to 1986 and from 2007 to 2012, where the amplitudes of the interannual variation are significantly higher. Using linear regression, the derived trends are estimated to be –3.73% per decade for SBA, –4.22% per decade for NT1 and –2.0% per decade for Hadley. The trends from SBA and NT1 differ slightly but provide similar trend information but that from Hadley is about half the other two, with a much more modest decline. The difference in the trend values for the Hadley data is likely due to the anomalous deviation of the data from the other two data sets as indicated in the preceding text. The corresponding estimates for the trends in sea ice area data are –4.35%, –4.71% and –2.8% per decade, respectively, all relatively higher than those for ice extent but again providing similar trend results for SBA and NT1 but a significantly lesser rate of decline for Hadley.

In the Antarctic, the trends are more modest and in the opposite direction as depicted in Figure 4.SM.2. Again, the patterns of the interannual variability are very similar for all three, with the Hadley data being the most different, exhibiting higher short-term fluctuations and a more positive trend. Trend results are +1.44%, +1.34% and +2.48% per decade for SBA, NT1 and Hadley, respectively. Again, the results from SBA and NT1 are slightly different but provide similar trend information while Hadley provides a considerably higher trend. The corresponding trends in ice area are +2.07%, +1.57% and +3.07% per decade, for SBA, NT1 and Hadley, respectively. The discrepancy in the trends for ice area between the SBA and NT1 results is in part due to lower concentration averages for NT1 compared with SBA data as indicated in the preceding text. However, they provide similar conclusions about the changes in the ice cover. The Hadley trend is again substantially higher than those of the other two.

For a more detailed comparison, September monthly sea ice extents for SBA, NT1 and Hadley for all years from 1979 to 2011 are plotted together in Figure 4.SM.3a. For completeness, ABA and NT2 ice extents using AMSR-E data are also shown for the period 2002–2011. The values from all three primary data sources are very similar, with the SBA showing the highest values and Hadley normally lowest. Values from AMSR-E data using ABA and NT2 are relatively lower because of higher resolution as discussed in Comiso and Nishio (2008), but otherwise there is good consistency. There are greater discrepancies among the three data sources when sea ice areas are plotted (Figure 4.SM.3b), with NT1 and Hadley showing good agreement up to 1997 and significant disagreement after that. The higher ice area values for SBA are associated with higher ice concentration values derived from the data than the other two, as discussed previously. The values for ABA and NT2 from AMSR-E (which have been used as the baseline) are in good agreement and also agree well with the SBA values. Large difference between NT1 and NT2 values are evident, as has been observed by Screen (2011). Nevertheless, the trends in extent for SBA and NT1 are –10.2% and –10.5% per decade, respectively, basically providing the same conclusion, while the trend in extent for the Hadley data is –8.0% per decade. The trends for ice area are also similar enough at –11.3% (SBA) and –12.5% per decade (NT1) while the trend for Hadley data is –10.2% per decade.

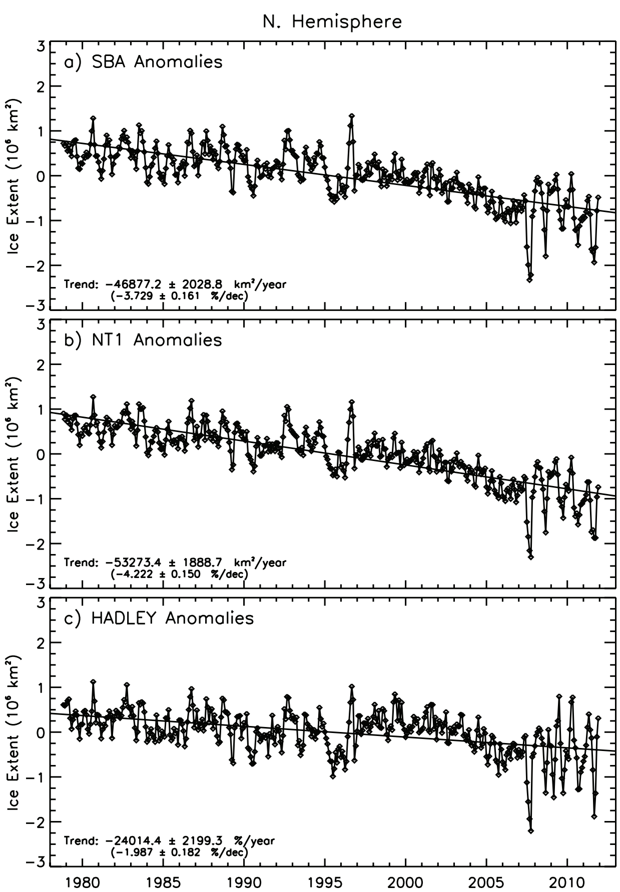

Figure 4.SM.1 | Monthly anomalies of ice extent from November 1978 to December 2011 using (a) SBA, (b) NT1 and (c) Hadley data in the Northern Hemisphere. Trends are shown with uncertainty calculated at 1 standard deviation (1σ).

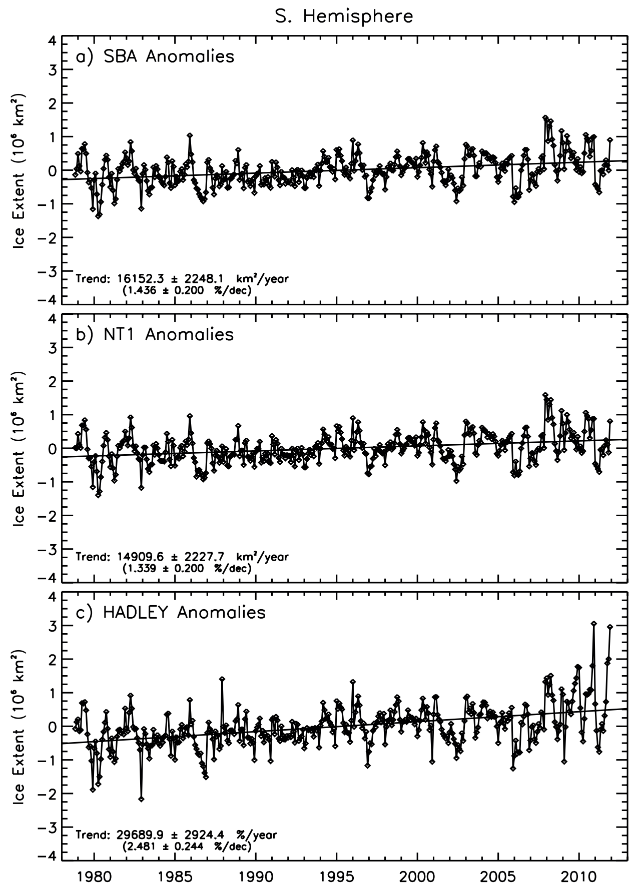

Figure 4.SM.2 | Monthly anomalies of ice extent from November 1978 to December 2011 using (a) SBA, (b) NT1 and (c) Hadley data in the Southern Hemisphere. Trends are shown with uncertainty calculated at 1 standard deviation (1σ).

Another data set that is available and has been used for sea ice studies is that from the Arctic Radiation and Turbulence Interaction Study (ARTIST) provided by the University of Bremen. The data make use of only the 89-GHz channels (horizontal and vertical polarized data) to generate relatively high resolution data from AMSR-E (5 to 6 km). High resolution is needed in many mesoscale studies. However, the 89-GHz radiation is very sensitive to weather and changes in the snow cover conditions, and the data should be used with care because they may be partly contaminated by incorrect values, especially under adverse weather conditions. Also, the ARTIST time series data from Aqua/AMSR-E is, as yet, too short for meaningful sea ice variability and trend studies.

Of the three satellite data sets that are currently available for sea ice variability and trend analysis, SBA and NT1 provides basically the same

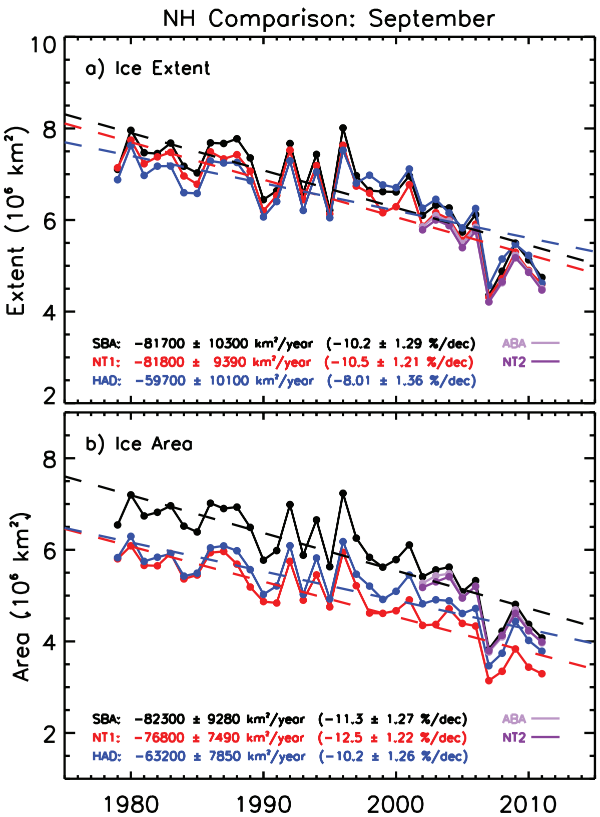

Figure 4.SM.3 | Monthly estimates of (a) sea ice extent and (b) sea ice area for the month of September from 1979 to 2011 for the Northern Hemisphere. Trends are shown with uncertainty calculated at 1 standard deviation (1σ).

patterns of interannual variability and approximately similar trends. The distributions are similar enough to provide basically the same information and conclusions about the trend of the changing sea ice cover. The patterns of variability provided by the Hadley data set are generally similar to those of SBA and NT1 but there are years when the data are suspect, as has been identified by Screen (2011). This is the primary reason for the discrepancies in the trends of the Hadley data compared with those of the SBA and NT1 data.

4.SM.2 Details of Studies of Glacier Area Change

Table 4.SM.1 provides an overview of studies reporting glacier area changes over entire mountain ranges or larger regions. Where available, area change rates are also given for sub-periods that have been extracted from the respective publications, partly using a linear extrapolation of given change rates to determine values for a common year in all sub-regions. In some studies, the glacier count is not given.

Table 4.SM.1 | Overview of studies presenting glacier area changes. **Bold** values in the column 'Change rate' indicate values shown in Figure 4.10. Values in *italics* refer to the entire period with 'Area covered' giving the value for the last year. Change rates are given for some regions to three decimals to avoid overlap of lines in Figure 4.10. For three regions (5, 9, and 12) studies on area changes were not found.

RGI Region	Country / Region	Sub-region / Mountain Range	Start Year	End Year	Number of Years	Glacier Count	Area Covered (km^2)	Relative Change (%)	Change Rate (% a^{-1})	Reference
1	USA, AK	Chugach Mountains	1952	2007	55	347	1285.7	–23	**–0.42**	Le Bris et al. (2011)
2	USA	North Cascades	1958	1998	40	321	117.3	–7.0	**–0.18**	Granshaw and Fountain (2006)
2	Canada	Rocky Mountains	1985	2001	16	523	1056.7	–7.6	–0.48	Tennant et al. (2012)
			2001	2006	5	523	976.5	–9.9	–1.98	
			1985	*2006*	*21*	*523*	*880.0*	*–16.7*	***–0.80***	
2	USA	Wind River Range	1966	2006	40	n/a	45.9	–37.7	**–0.94**	Thompson et al. (2011)
2	Canada	Yukon	1959	2007	48	n/a	11622	–21.9	**–0.456**	Barrand and Sharp (2010)
2	Canada	Rocky Mountains[a]	1985	2005	20	14329	30063	–11.1	**–0.555**	Bolch et al. (2010)
2	Canada	Clemenceau Icefield	1985	2001	16	123	313	–13.4	**–0.84**	Jiskoot et al. (2009)
		Chaba Group	1985	2001	16	53	97	–28.9	**–1.81**	
2	Canada	Rocky Mountains	1952	2001	49	59	40	–15	**–0.31**	Debeer and Sharp (2007)
		Columbia Mountains	1952	2001	49	403	397	–5.0	**–0.10**	
		Coast Mountains	1964	2002	38	1053	2397	–5.0	**–0.13**	
3	Canada	Queen Elizabeth Island	1960	2000	40	1274	107071	–2.7	**–0.07**	Sharp et al. (2013)
3	Canada	North Ellesmere	1960	2000	40	473	27556	–3.4	–0.09	Sharp et al. (2013)
		Agassiz	1960	2000	40	296	21645	–1.3	–0.03	
		Axel/Meighen / Melville	1960	2000	40	165	12231	–1.7	–0.04	
		Prince of Wales	1960	2000	40	39	19558	–0.9	–0.02	
		South Ellesmere	1960	2000	40	187	10696	–5.9	–0.15	
		Devon Island	1960	2000	40	114	15344	–4.0	–0.10	
4	Canada	Bylot Island	1959	2001	42	n/a	5036	–5.0	**–0.119**	Dowdeswell et al. (2007)
4	Canada	Barnes Ice Cap	1958	2000	42	n/a	5995	–2.0	**–0.048**	Sharp et al. (2013)
		Penny Ice Cap	1959	2000	41	n/a	6604	–1.9	**–0.046**	
		Terra Nivea	1958	2000	42	n/a	197	–14.0	**–0.33**	
		Grinnel Ice Cap	1958	2000	42	n/a	135	–10.9	**–0.26**	
4	Canada	Baffin Island	1975	2000	25	264	2187	–12.5	**–0.16**	Paul and Svoboda (2009)
5	Greenland	n/a								
6	Iceland	Four ice caps	1998	2011	13	4	1004.5	–7.6	**–0.58**	Johannesson et al. (2013)
7	Svalbard	Glaciers >1 km^2	1990	2008	18	n/a	5204.7	–4.6	**–0.26**	König et al. (2013)
8	Norway	Jostedalbreen	1966	2006	40	297	725.1	–9	**–0.225**	Paul et al. (2011)
8	Norway	Jotunheimen	1965	2003	38	164	229.5	–12.4	**–0.33**	Andreassen et al. (2008)
8	Norway	Svartisen	1968	1999	31	300	518.0	–1.1	**–0.04**	Paul and Andreassen (2009)
9	Russian Arctic	n/a								
10	Russian Federation	Ural	1956	2000	44	30	9.17	–22.3	**–0.51**	Shahgedanova et al. (2012)
10	Russian Federation	Kodar Mountains	1995	2001	6	34	11.72	–18.7	–3.11	Stokes et al. (2013)
			2001	2010	9	34	9.53	–26.4	–2.94	
			1995	*2010*	*15*	*34*	*7.01*	*–40.2*	*–2.68*	
10	Russian Federation	Altai Chuya Ridges	1952	2004	52	126	284	–19.7	**–0.38**	Shahgedanova et al. (2010)
10	Russian Federation	Altai	1952	2008	56	1030	805	–10.2	**–0.182**	Narozhniy and Zemtsov (2011)
11	Austria	Alps	1969	1998	29	925	567	–17.1	**–0.59**	Lambrecht and Kuhn (2007)
11	Austria	Ötztaler Alps	1997	2006	9	81	116	–8.2	**–0.9**	Abermann et al. (2009)
11	Switzerland	Alps	1973	1999	26	938	1171.2	–16.1	**–0.62**	Paul et al. (2004)
			1985	1998	13	471	372.2	–18.0	**–1.38**	
11	Spain	Pyrenees	1982	1994	12	10	6.08	–20.9	–1.97	Gonzales Trueba et al. (2008)
			1994	2001	7	10	4.81	–39.7	–5.6	
			1982	*2001*	*19*	*10*	*6.08*	*–52.3*	*–2.75*	

(continued on next page)

Table 4.SM.1 (continued)

RGI Region	Country / Region	Sub-region / Mountain Range	Start Year	End Year	Number of Years	Glacier Count	Area Covered (km²)	Relative Change (%)	Change Rate (% a⁻¹)	Reference
11	Italy	Aosta Valley	1975	1999	24	174	163.9	–16.7	–0.7	Diolaiuti et al. (2012)
			1999	2005	6	174	136.6	–12.4	–2.07	
			1975	*2005*	*30*	*174*	*119.6*	*–27.0*	***–0.9***	
11	Italy	South Tyrol	1983	1997	14	205	136.6	–19.7	–1.41	Knoll and Kerschner (2009)
			1997	2006	9	302	109.7	–11.9	–1.32	
			1983	2006	23	205	136.6	–31.6	**–1.37**	
11	Italy	Lombardy	1992	1999	7	249	117.4	–10.8	–1.54	Citterio et al. (2007)
12	Caucasus	n/a								
13	Mongolia	Altai Mountains	1989	2009	20	n/a	213	–4.2	**–0.21**	Krumwiede et al. (2013)
13	China	Muztag Ata and Konggur Mountains (East Pamir)	1962	1990	28	n/a	838.2	–3.4	–0.12	Shangguan et al. (2006)
			1990	1999	9	n/a	809.9	–4.6	–0.52	
			1962	*1999*	*37*		*772.2*	*–7.9*	***–0.214***	
13	China (Tarim Basin)	Quarqan	1977	2001	24	399	752.6	–3.4	**–0.14**	Shangguan et al. (2009)
		Keliya	1970	1999	29	731	1306.5	–3.1	**–0.11**	
		Hotan	1968	2000	32	2487	5131.8	–0.7	**–0.02**	
		Yarkant	1974	2001	27	1421	3170.6	–6.1	**–0.23**	
		Pamir	1964	2001	37	880	2085.4	–7.9	**–0.21**	
		Tienshan	1964	2000	36	1249	4039.2	–1.3	**–0.04**	
		Kaidu	1964	2000	36	498	405.8	–7.1	**–0.20**	
13	China (Tibet)	Gongga Mountains	1966	1989	23	74	257.7	–5.8	–0.25	Pan et al. (2012b)
			1989	2009	20	75	242.8	–5.9	–0.29	
			1966	*2009*	*43*	*76*	*228.5*	*–11.3*	***–0.26***	
13	Kyrgistan	Pskem	1968	2000	32	525	219.8	–19.47	–0.61	Narama et al. (2010)
			2000	2007	7	525	177.0	–6.69	**–0.96**	
		Ili-Kungoy	1971	1999	28	735	672.2	–12.18	–0.44	
			1999	2007	8	735	590.3	–4.12	**–0.52**	
		At-Bashi	1968	2000	32	192	113.6	–12.06	–0.38	
			2000	2007	7	192	99.9	–4.20	**–0.60**	
		SE-Fergana	1968	2000	32	306	190.1	–9.21	–0.29	
			2000	2007	7	306	172.6	–0.52	**–0.07**	
13	China	Qilian Mountains[a]	1956	2003	47	910	397.4	–21.7	**–0.462**	Wang et al. (2011)
13	China	Karlik Shan	1971	1992	21	n/a	126	–2.63	–0.13	Wang et al. (2009)
			1992	2001	9	n/a	122.7	–2.67	–0.27	
			1971	*2001*	*30*	*n/a*	*119.4*	*5.2*	***–0.17***	
13	China	Lenglongling[a]	1972	2007	35	179	86.2	–28.3	**–0.81**	Pan et al. (2012a)
13	Kyrgistan	Akshiirak	1977	2003	26	178	406.8	–8.6	**–0.33**	Aizen et al. (2007)
		Ala Archa	1981	2003	22	48	40.62	–10.6	**–0.48**	
14	Himalaya	Ten basins mean[a]	1962	2004	42	1868	6332	–15.8	**–0.38**	Kulkarni et al. (2011)
14	India	Kang Yatze	1969	1991	23	121	96.4	–13.0	–0.56	Schmidt and Nusser (2012)
			1991	2010	18	121	83.9	–1.5	–0.09	
			1969	*2010*	*41*	*121*	*96.4*	*–14.4*	***–0.35***	
14	India	Gharwal Himalaya[a]	1968	2006	38	82	600	–4.6	**–0.121**	Bhambri et al. (2011)
15	Nepal	Khumbu Himal	1976	2006	30	n/a	3211.9	–15.6	**–0.52**	Nie et al. (2010)
15	Nepal	Khumbu Himal	1962	2005	43	n/a	92.3	–5.3	**–0.123**	Bolch et al. (2008)
15	Nepal	Sagarmatha National Park	1962	2001	39	29	403.9	–4.9	**–0.126**	Salerno et al. (2008)

(continued on next page)

Table 4.SM.1 (continued)

RGI Region	Country / Region	Sub-region / Mountain Range	Start Year	End Year	Number of Years	Glacier Count	Area Covered (km²)	Relative Change (%)	Change Rate (% a⁻¹)	Reference
16	Peru	Cordillera Coropuna	1955	2003	48	711	123	–54	**–1.125**	Silverio and Jaquet (2012)Peru
16	Peru	Cordillera Blanca	1970	1990	20	n/a	190	–12.8	–0.64	Baraer et al. (2012)
			1990	2009	19		165	–17.4	–0.92	
			1970	*2009*	*39*		*136.3*	*–28.0*	***–0.72***	
16	Peru	Cordillera Vilcanota	1985	1996	11	n/a	444	–22.5	–2.05	Salzmann et al. (2013)
			1996	2006	10		344	–13.7	–1.37	
			1985	*2006*	21		*297*	*–33.2*	***–1.58***	
16	Peru	Quelcaya Ice Cap	1985	2000	15	n/a	55.7	–17.6	–1.17	Salzmann et al. (2013)
			2000	2009	9		45.9	–3.1	–0.34	
			1985	*2009*	*24*		*42.8*	*–23.1*	***–0.96***	
16	Indonesia	Puncack Jaya	1942	1972	30	10	9.9	–30.3	–1.01	Klein and Kincaid (2006)
			1972	2002	30	5	6.9	–66.2	–2.23	
			1942	*2002*	*60*		2.15	–78.3	***–1.30***	
16	Columbia	Six mountain ranges[a]	1959	1987	28	n/a	106.8	–21.9	–0.78	Ceballos et al. (2006)
			1987	2002	15		83.5	–33.5	–2.23	
			1959	*2002*	*43*		*45.6*	*–48.1*	***–1.18***	
16	Peru	Cordillera Blanca	1970	2003	33	445	665.1	–22.4	**–0.68**	Racoviteanu et al. (2008)
16	Tansania	Kilimandscharo[a]	1962	2011	49	n/a	7.32	–76.0	**–1.55**	Cullen et al. (2013)
17	Chile	Gran Campo Nevado	1942	2002	60	81	252.6	–14.4	**–0.24**	Schneider et al. (2007)
17	Chile / Argentina	San Lorenzo Mountains	1985	2000	15	213	239.0	–9.9	–0.66	Falaschi et al. (2013)
			2000	2008	8	213	215.4	–9.7	–1.21	
			1985	*2008*	*23*	*213*	*206.9*	*–13.4*	***–0.58***	
17	Chile / Argentina	Patagonia	1986	2001	15	183	23743	–2.2	–0.14	Davies and Glasser (2012)
			2001	2011	10	165	23229	–2.2	–0.22	
			1986	*2011*	*25*	*183*	*22717*	*–4.3*	***–0.17***	
17	Chile	Northern Patagonia Icefield	1979	2001	22	>70[b]	4093	–3.4	**–0.15**	Rivera et al. (2007)
17	Chile	Aconcagua Basin	1955	2003	48		151	–19.9	**–0.41**	Bown et al. (2008)
18	New Zealand	Southern Alps	1978	2002	24	n/a	513	–16.6	**–0.69**	Gjermundsen et al. (2011)
19	Antarctica	Kerguelen Island[a]	1963	2001	38	n/a	703	–21	**–0.55**	Berthier et al. (2009)
19	Antarctica	King George Island	1956	1995	39	n/a	1250	–7.0	**–0.179**	Rückamp et al. (2011)
			2000	2008	8	n/a		–1.6	**–0.20**	

Notes:

(a) More detailed analyses (e.g., sub-regions, other periods) are available in the respective papers.

(b) Glaciers <0.5 km² were not counted separately.

References

Abermann, J., A. Lambrecht, A. Fischer, and M. Kuhn, 2009: Quantifying changes and trends in glacier area and volume in the Austrian Otztal Alps (1969–1997–2006). *Cryosphere*, **3**, 205–215.

Aizen, V. B., V. A. Kuzmichenok, A. B. Surazakov, and E. M. Aizen, 2007: Glacier changes in the Tien Shan as determined from topographic and remotely sensed data. *Global Planet. Change*, **56**, 328–340.

Andreassen, L. M., F. Paul, A. Kaab, and J. E. Hausberg, 2008: Landsat-derived glacier inventory for Jotunheimen, Norway, and deduced glacier changes since the 1930s. *Cryosphere*, **2**, 131–145.

Baraer, M., et al., 2012: Glacier recession and water resources in Peru's Cordillera Blanca. *J. Glaciol.*, **58**, 134–150.

Barrand, N. E., and M. J. Sharp, 2010: Sustained rapid shrinkage of Yukon glaciers since the 1957–1958 International Geophysical Year. *Geophys. Res. Lett.*, **37,** L07501.

Berthier, E., R. Le Bris, L. Mabileau, L. Testut, and F. Remy, 2009: Ice wastage on the Kerguelen Islands (49 degrees S, 69 degrees E) between 1963 and 2006. *J. Geophys. Res. Earth Surf.*, **114**, 11.

Bhambri, R., T. Bolch, R. K. Chaujar, and S. C. Kulshreshtha, 2011: Glacier changes in the Garhwal Himalaya, India, from 1968 to 2006 based on remote sensing. *J. Glaciol.*, **57,** 543-556.

Bolch, T., B. Menounos, and R. Wheate, 2010: Landsat-based inventory of glaciers in western Canada, 1985–2005. *Remote Sens. Environ.*, **114**, 127–137.

Bolch, T., M. Buchroithner, T. Pieczonka, and A. Kunert, 2008: Planimetric and volumetric glacier changes in the Khumbu Himal, Nepal, since 1962 using Corona, Landsat TM and ASTER data. *J. Glaciol.*, **54**, 592–600.

Bown, F., A. Rivera, and C. Acuna, 2008: Recent glacier variations at the Aconcagua basin, central Chilean Andes. *Ann. Glaciol.,* **48**, 43–48.

Cavalieri, D. J., and C. L. Parkinson, 2012: Arctic sea ice variability and trends, 1979–2010. *Cryosphere*, **6**, 957–979.

Cavalieri, D. J., P. Gloersen, and W. J. Campbell, 1984: Determination of sea ice parameters with the Nimbus-7 SMMR. *J. Geophys. Res. Atmos.*, **89**, 5355–5369.

Ceballos, J. L., C. Euscategui, J. Ramirez, M. Canon, C. Huggel, W. Haeberli, and H. Machguth, 2006: Fast shrinkage of tropical glaciers in Colombia. *Ann. Glaciol.,* **43***,* 194–201.

Citterio, M., G. Diolaiuti, C. Smiraglia, C. D'Agata, T. Carnielli, G. Stella, and G. B. Siletto, 2007: The fluctuations of Italian glaciers during the last century: A contribution to knowledge about Alpine glacier changes. *Geograf. Annal. A*, **89A**, 167–184.

Comiso, J. C., 1986: Characteristics of winter sea ice from satellite multispectreal microwave observations *J. Geophys. Res. Oceans*, **91**, 975–994.

Comiso, J. C., and F. Nishio, 2008: Trends in the sea ice cover using enhanced and compatible AMSR-E, SSM/I, and SMMR data. *J. Geophys. Res. Oceans*, **113**, C02S07.

Comiso, J. C., and C. L. Parkinson, 2008: Arctic sea ice parameters from AMSR-E using two techniques, and comparisons with sea ice from SSM/I. *J. Geophys. Res.*, **113**, C02S05.

Cullen, N. J., P. Sirguey, T. Moelg, G. Kaser, M. Winkler, and S. J. Fitzsimons, 2013: A century of ice retreat on Kilimanjaro: The mapping reloaded. *Cryosphere*, **7**, 419–431.

Davies, B. J., and N. F. Glasser, 2012: Accelerating shrinkage of Patagonian glaciers from the "Little Ice Age" (c. AD 1870) to 2011. *J. Glaciol.*, **58**, 1063–1084.

Debeer, C. M., and M. J. Sharp, 2007: Recent changes in glacier area and volume within the southern Canadian Cordillera. *Ann. Glaciol.,* **46**, 215–221.

Diolaiuti, G. A., D. Bocchiola, M. Vagliasindi, C. D'Agata, and C. Smiraglia, 2012: The 1975–2005 glacier changes in Aosta Valley (Italy) and the relations with climate evolution. *Prog. Phys. Geogr.*, **36**, 764–785.

Dowdeswell, E. K., J. A. Dowdeswell, and F. Cawkwell, 2007: On the glaciers of Bylot Island, Nunavut, Arctic Canada. *Arct. Antarct. Alp. Res.*, **39**, 402-411.

Falaschi, D., C. Bravo, M. Masiokas, R. Villalba, and A. Rivera, 2013: First glacier inventory and recent changes in glacier area in the Monte San Lorenzo Region (47°S), Southern Patagonian Andes, South America. *Arct. Antarct. Alp. Res.*, **45**, 19–28.

Gjermundsen, E. F., R. Mathieu, A. Kääb, T. Chinn, B. Fitzharris, and J. O. Hagen, 2011: Assessment of multispectral glacier mapping methods and derivation of glacier area changes, 1978–2002, in the central Southern Alps, New Zealand, from ASTER satellite data, field survey and existing inventory data. *J. Glaciol.*, **57**, 667–683.

Gloersen, P., W. J. Campbell, D. J. Cavalieri, J. C. Comiso, C. L. Parkinson, and H. J. Zwally, 1993: Satellite passive microwave observations and analysis of Arctic and Antarctic sea-ice. *Ann. Glaciol.*, **17**, 149–154.

Gonzales Trueba, J. J., R. Martin Moreno, E. Martinez de Pison, and E. Serrano, 2008: Little Ice Age' glaciation and current glaciers in the Iberian Peninsula. *Holocene*, **18**, 551–568.

Granshaw, F. D., and A. G. Fountain, 2006: Glacier change (1958–1998) in the North Cascades National Park Complex, Washington, USA. *J. Glaciol.*, **52**, 251–256.

Jiskoot, H., C. J. Curran, D. L. Tessler, and L. R. Shenton, 2009: Changes in Clemenceau Icefield and Chaba Group glaciers, Canada, related to hypsometry, tributary detachment, length-slope and area-aspect relations. *Ann. Glaciol.*, **50**, 133–143.

Johannesson, T., et al., 2013: Ice-volume changes, bias estimation of mass-balance measurements and changes in subglacial lakes derived by lidar mapping of the surface of Icelandic glaciers. *Ann. Glaciol.*, **54**, 63–74.

Klein, A. G., and J. L. Kincaid, 2006: Retreat of glaciers on Puncak Jaya, Irian Jaya, determined from 2000 and 2002 IKONOS satellite images. *J. Glaciol.*, **52**, 65–79.

Knoll, C., and H. Kerschner, 2009: A glacier inventory for South Tyrol, Italy, based on airborne laser-scanner data. *Ann. Glaciol.*, **50**, 46–52.

König, M., C. Nuth, J. Kohler, G. Moholdt, and R. Pettersson, 2013: A digital glacier database for Svalbard. In: *Global Land Ice Measurements form Space* [J. S. Kargel, G. J. Leonard, M. P. Bishop, A. Kääb and B. Raup (eds.)]. Springer Praxis, New York, NY, USA, 229-239.

Krumwiede, B. S., U. Kamp, G. J. Leonard, A. Dashtseren, and M. Walther, 2013: Recent glacier changes in the Mongolian Altai Mountains: Case studies from Munkh Khairkhan and Tavan Bogd. In: *Global Land Ice Measurements from Space* [J. S. Kargel, G. J. Leonard, M. P. Bishop, A. Kääb and B. Raup (eds.)]. Springer-Praxis, New York, NY, USA, 481-507.

Kulkarni, A. V., B. P. Rathore, S. K. Singh, and I. M. Bahuguna, 2011: Understanding changes in the Himalayan cryosphere using remote sensing techniques. *Int. J. Remote Sens.*, **32**, 601–615.

Lambrecht, A., and M. Kuhn, 2007: Glacier changes in the Austrian Alps during the last three decades, derived from the new Austrian glacier inventory. *Ann. Glaciol.,* **46**, 177–184.

Le Bris, R., F. Paul, H. Frey, and T. Bolch, 2011: A new satellite-derived glacier inventory for western Alaska. *Ann. Glaciol.*, **52**, 135-143.

Markus, T., and D. J. Cavalieri, 2000: An enhancement of the NASA Team sea ice algorithm. *IEEE Trans. Geosci. Remote Sens.*, **38**, 1387–1398.

Narama, C., A. Kaab, M. Duishonakunov, and K. Abdrakhmatov, 2010: Spatial variability of recent glacier area changes in the Tien Shan Mountains, Central Asia, using Corona (similar to 1970), Landsat (similar to 2000), and ALOS (similar to 2007) satellite data. *Global Planet. Change*, **71**, 42–54.

Narozhniy, Y., and V. Zemtsov, 2011: Current state of the Altai Glaciers (Russia) and trends over the period of instrumental observations 1952–2008. *Ambio*, **40**, 575-588.

Nie, Y., Y. L. Zhang, L. S. Liu, and J. P. Zhang, 2010: Glacial change in the vicinity of Mt. Qomolangma (Everest), central high Himalayas since 1976. *J. Geograph. Sci.*, **20**, 667–686.

Pan, B., B. Cao, J. Wang, G. Zhang, C. Zhang, Z. Hu, and B. Huang, 2012a: Glacier variations in response to climate change from 1972 to 2007 in the western Lenglongling mountains, northeastern Tibetan Plateau. *J. Glaciol.*, **58**, 879–888.

Pan, B. T., G. L. Zhang, J. Wang, B. Cao, H. P. Geng, C. Zhang, and Y. P. Ji, 2012b: Glacier changes from 1966–2009 in the Gongga Mountains, on the south-eastern margin of the Qinghai-Tibetan Plateau and their climatic forcing. *Cryosphere*, **6**, 1087–1101.

Parkinson, C. L., and J. C. Comiso, 2008: Antarctic sea ice parameters from AMSR-E data using two techniques and comparisons with sea ice from SSM/I. *J. Geophys. Res. Oceans*, **113**, C02S06.

Parkinson, C. L., and D. J. Cavalieri, 2012: Antarctic Sea Ice Variability and Trends, 1979–2010. *Cryosphere*, **6**, 871–880.

Parkinson, C. L., D. J. Cavalieri, P. Gloersen, H. J. Zwally, and J. C. Comiso, 1999: Arctic sea ice extents, areas, and trends, 1978–1996. *J. Geophys. Res. Oceans*, **104**, 20837–20856.

Parkinson, C. L., J. C. Comiso, H. J. Zwally, D. J. Cavalieri, P. Gloersen, and W. Campbell, 1987: Analysis of northern hemisphere sea ice from satellite passive microwave data. *Ann. Glaciol.*, **9**, 1–8.

Paul, F., and L. M. Andreassen, 2009: A new glacier inventory for the Svartisen region, Norway, from Landsat ETM plus data: challenges and change assessment. *J. Glaciol.*, **55**, 607–618.

Paul, F., and F. Svoboda, 2009: A new glacier inventory on southern Baffin Island, Canada, from ASTER data: II. Data analysis, glacier change and applications. *Ann. Glaciol.*, **50**, 22–31.

Paul, F., L. M. Andreassen, and S. H. Winsvold, 2011: A new glacier inventory for the Jostedalsbreen region, Norway, from Landsat TM scenes of 2006 and changes since 1966. *Ann. Glaciol.*, **52**, 153-162.

Paul, F., A. Kaab, M. Maisch, T. Kellenberger, and W. Haeberli, 2004: Rapid disintegration of Alpine glaciers observed with satellite data. *Geophys. Res. Lett.*, **31**, 4.

Racoviteanu, A. E., Y. Arnaud, M. W. Williams, and J. Ordonez, 2008: Decadal changes in glacier parameters in the Cordillera Blanca, Peru, derived from remote sensing. *J. Glaciol.*, **54**, 499–510.

Rayner, N. A., et al., 2003: Global analyses of SST, sea ice and night marine air temperature since the late nineteenth century. *J. Geophys. Res.*, **108**, 4407.

Rivera, A., T. Benham, G. Casassa, J. Bamber, and J. A. Dowdeswell, 2007: Ice elevation and areal changes of glaciers from the Northern Patagonia Icefield, Chile. *Global Planet. Change*, **59**, 126–137.

Rückamp, M., M. Braun, S. Suckro, and N. Blindow, 2011: Observed glacial changes on the King George Island ice cap, Antarctica, in the last decade. *Global Planet. Change*, **79**, 99–109.

Salerno, F., E. Buraschi, G. Bruccoleri, G. Tartari, and C. Smiraglia, 2008: Glacier surface-area changes in Sagarmatha national park, Nepal, in the second half of the 20th century, by comparison of historical maps. *J. Glaciol.*, **54**, 738–752.

Salzmann, N., C. Huggel, M. Rohrer, W. Silverio, B. G. Mark, P. Burns, and C. Portocarrero, 2013: Glacier changes and climate trends derived from multiple sources in the data scarce Cordillera Vilcanota region, southern Peruvian Andes. *Cryosphere*, **7**, 103–118.

Schmidt, S., and M. Nusser, 2012: Changes of High Altitude Glaciers from 1969 to 2010 in the Trans-Himalayan Kang Yatze Massif, Ladakh, Northwest India. *Arct. Antarct. Alp. Res.*, **44**, 107–121.

Schneider, C., M. Schnirch, C. Acuna, G. Casassa, and R. Kilian, 2007: Glacier inventory of the Gran Campo Nevado Ice Cap in the Southern Andes and glacier changes observed during recent decades. *Global Planet. Change*, **59**, 87–100.

Screen, J. A., 2011: Sudden increase in Antarctic sea ice: Fact or artifact? *Geophys. Res. Lett.*, **38**, L13702.

Shahgedanova, M., G. Nosenko, T. Khromova, and A. Muraveyev, 2010: Glacier shrinkage and climatic change in the Russian Altai from the mid-20th century: An assessment using remote sensing and PRECIS regional climate model. *J. Geophys. Res. Atmos.*, **115**, 12.

Shahgedanova, M., G. Nosenko, I. Bushueva, and M. Ivanov, 2012: Changes in area and geodetic mass balance of small glaciers, Polar Urals, Russia, 1950–2008. *J. Glaciol.*, **58**, 953–964.

Shangguan, D., S. Liu, Y. Ding, L. Ding, J. Xu, and L. Jing, 2009: Glacier changes during the last forty years in the Tarim Interior River basin, northwest China. *Prog. Nat. Sci.*, **19**, 727–732.

Shangguan, D., et al., 2006: Monitoring the glacier changes in the Muztag Ata and Konggur mountains, east Pamirs, based on Chinese Glacier Inventory and recent satellite imagery. *Ann. Glaciol.*, **43**, 79–85.

Sharp, M., et al., 2013: Remote Sensing of Recent Glacier Changes in the Canadian Arctic. In: *Global Land Ice Measurements from Space* [J. S. Kargel, G. J. Leonard, M. P. Bishop, A. Kääb and B. Raup (eds.)]. Springer-Praxis, New York, NY, USA, in press.

Silverio, W., and J.-M. Jaquet, 2012: Multi-temporal and multi-source cartography of the glacial cover of Nevado Coropuna (Arequipa, Peru) between 1955 and 2003. *Int. J. Remote Sens.*, **33**.

Stammerjohn, S. E., D. G. Martinson, R. C. Smith, X. Yuan, and D. Rind, 2008: Trends in Antarctic annual sea ice retreat and advance and their relation to El Niño-Southern Oscillation and Southern Annular Mode variability. *J. Geophys. Res. Oceans*, **113**, C03S90.

Steffen, K., D. J. Cavalieri, J. C. Comiso, K. St Germain, P. Gloersen, J. Key, and I. Rubinstein, 1992: The estimation of geophysical parameters using Passive Microwave Algorithms. In: *Microwave Remote Sensing of Sea Ice* [F. D. Carsey (ed.)]. American Geophysical Union, Washington, DC, pp. 201–231.

Stokes, C. R., M. Shahgedanova, I. S. Evans, and V. V. Popovnin, 2013: Accelerated loss of alpine glaciers in the Kodar Mountains, south-eastern Siberia. *Global Planet. Change*, **101**, 82–96.

Stroeve, J., M. M. Holland, W. Meier, T. Scambos, and M. Serreze, 2007: Arctic sea ice decline: Faster than forecast. *Geophys. Res. Lett.*, **34**, L09501.

Svendsen, E., et al., 1983: Norvegian Remote-Sensing Experiment—Evaluation of the NIMBUS-7 Scanning Multichannel Microwave Radiometer for Sea Ice Research. *J. Geophys. Res. Oceans Atmos.*, **88**, 2781–2791.

Swift, C. T., L. S. Fedor, and R. O. Ramseier, 1985: An algorithm to measure sea ice concentration with microwave radiometers. *J. Geophys. Res. Oceans*, **90**, 1087–1099.

Tennant, C., B. Menounos, R. Wheate, and J. J. Clague, 2012: Area change of glaciers in the Canadian Rocky Mountains, 1919 to 2006. *Cryosphere*, **6**, 1541–1552.

Thompson, D., G. Tootle, G. Kerr, R. Sivanpillai, and L. Pochop, 2011: Glacier variability in the Wind River Range, Wyoming. *J. Hydrol. Engng.*, **16**, 798-805.

Walsh, J. E., and W. L. Chapman, 2001: 20th-century sea-ice variations from observational data. *Ann. Glaciol.,* **33**, 444–448.

Wang, P., Z. Li, and W. Gao, 2011: Rapid Shrinking of Glaciers in the Middle Qilian Mountain Region of Northwest China during the Last similar to 50 Years. *J. Earth Sci.*, **22**, 539–548.

Wang, Y. T., S. G. Hou, and Y. P. Liu, 2009: Glacier changes in the Karlik Shan, eastern Tien Shan, during 1971/72–2001/02. *Ann. Glaciol.*, **50**, 39–45.

Zwally, H. J., C. L. Parkinson, and J. C. Comiso, 1983: Variability of Antarctic sea ice and changes in carbon dioxide. *Science*, **220**, 1005–1012.

Zwally, H. J., J. C. Comiso, C. L. Parkinson, D. J. Cavalieri, and P. Gloersen, 2002: Variability of Antarctic sea ice 1979–1998. *J. Geophys. Res.*, **107**, 1029–1047.